REVIEW ARTICLE

Multistage Auto-ignition of Undiluted Methane/Air Mixtures under Engine-relevant Condition

Yingjia Zhang[1]*, Wuchuan Sun[1], Wenlin Huang[1], Xiaokang Qin[1], Jinshu Liu[1], Bensi Dong[2], Yongkai Quan[2]*, Zuohua Huang[1]

[1]State Key Laboratory of Multiphase Flow in Power Engineering, Xi'an Jiaotong University, Xi'an 710049, China,

[2]National Key Laboratory of Science and Technology on Aero-Engine Aero-thermodynamics, School of Energy and Power Engineering, Beihang University, Beijing 100083, China

Abstract: Gas-phase auto-ignition delay times (IDTs) of methane/"air" (21% O_2/79% Ar) mixtures were measured behind reflected shock waves, using a kinetic shock tube. Experiments were performed at fixed pressure of 1.8 MPa and equivalence ratios of 0.5 and 1.0, over the temperature range of 800–1000 K. Overall, the effect of equivalence ratio on IDT is negligible at entire temperatures measured in this study. The difference from traditional ignition regime at high temperatures, the undiluted methane/air mixtures present a four-stage ignition process at lower temperatures, namely deflagration delay, deflagration, deflagration-detonation transition, and detonation. Four popular kinetic mechanisms, UBC Mech 2.1, GRI Mech 3.0, Aramco Mech 2.0, and USC Mech 2.0, were used to simulate the new measurements. Only UBC Mech 2.1 showed satisfactory predictions in the reactivity of the undiluted methane mixtures; it was, thus, adopted to perform sensitivity analysis for identifying dominant reactions in the ignition process. The difference in channels contributing ȮH radicals causes a reduced global activation energy with decreasing temperatures.

Keywords: Methane; multistage ignition; shock tube; sensitivity analysis

*Correspondence to: Yingjia Zhang, State Key Laboratory of Multiphase Flow in Power Engineering, Xi'an Jiaotong University, Xi'an 710049, China, yjzhang_xjtu@xjtu.edu.cn; Yongkai Quan, National Key Laboratory of Science and Technology on Aero-Engine Aero-thermodynamics, School of Energy and Power Engineering, Beihang University, Beijing 100083, China, quanyongkai@126.com

Received: November 11, 2018; **Accepted:** April 4, 2019; **Published Online:** May 2, 2019

Citation: Zhang Y, Sun W, Huang W, Qin X, Liu J, Dong B, Quan Y, Huang Z. Multistage auto-ignition of undiluted methane/air mixtures under engine-relevant condition. J Chem Res Appl, 2(1): 898. http://dx.doi.org/10.18063/jcra.v2n1.898

1. Introduction

Methane, principle component of natural gas, is a popular reference fuel for internal combustion engines[1], gas turbines[2], and propulsion application[3]. The increasing popularity of natural gas in those real engines raises the importance of predicting auto-ignition behavior of methane under practical engine conditions. Ignition and oxidation of methane have been, therefore, investigated over the past five decades[4-18]. It should be said that the research has completely covered pressures from the environment to supercritical conditions over low- to high-temperatures. During this period, many detailed mechanisms have been developed, typically, UBC Mech 2.1[12,19,20], GRI Mech 3.0[21], Aramco Mech 2.0[22-25], and USC Mech 2.0[26], to characterize the ignition, oxidation, and combustion of methane.

As clearly reported in literature that increasing pressure shows promoting effect on the ignition delay times of methane and this tendency is in line with different shock tube experiments. However, the temperature-dependence of IDT presents a revised "S" shape with decreasing temperatures observed in the work of Huang *et al.*[12], and the similar phenomenon

doi: http://dx.doi.org/10.18063/jcra.v2n1.898

was also observed by Petersen *et al*.[10,11]. In general, the global activation of methane is in between 43 and 52 kcal/mol reported in literature under high temperatures and low pressures[4,27,28]. In the work of Huang *et al*.[12], however, they found that the activation energy fitted by the experimental data was 16 kcal/mol at temperatures between 1200 K and 1300 K. It decreases by 13 kcal/mol at the temperatures of 1100–1200 K but increases by 18 kcal/mol at the temperatures <1100 K. The reason causing the change in activation energy is due mainly to the different kinetic regimes at various temperatures. At lower temperatures, the primary reaction to consume CH_3 radicals is $CH_3 + O_2 = CH_3O_2$, following by the chain branching reaction $CH_3O_2 + CH_3 = 2CH_3O$. The two parallel reactions accelerate the conversion of CH_3 to CH_3O, leading to an obvious promotion in the auto-ignition and reduction in the activation energy. Huang *et al*.[12] indicated that this nonlinear temperature-dependence of IDT was more pronounced at fuel-stoichiometric condition than at fuel-lean condition. Moreover, GRI Mech 3.0[21] was not capable of predicting the transition of activation energy for methane oxidation at high pressures.

Unfortunately, most of the research provides IDT data, and rather limited pressure-time histories are available in literature. It is no doubt difficult to have an insight into the detail of auto-ignition process of methane at engine relevant conditions. The first aim of this study is, therefore, to detect the IDTs for methane/air mixtures with pressure profiles. The second aim is to compare the experimental measurements to model simulations with different kinetic mechanisms, not only for total IDT but also for auto-ignition pressure traces, so that it can verify whether the current models are suitable for computational fluid mechanics simulation of engine combustors.

2. Experimental approach

2.1. Shock tube

IDTs and pressure-time histories of various methane/air mixtures were detected behind the reflected shock waves using the kinetic shock tube at Xi'an Jiaotong University. Details of the facility are available in our previous work[27-29]. Briefly, 4.0 m long driver-section and 4.3 m long driven-section are separated by two polyethylene terephthalate diaphragms, with an inner diameter of 11.5 cm of the tube, Figure 1. Helium was used as the driver gas and typical test times with uniform conditions were 2 ms. However, the test time for the shock tube was further extended to 6 ms when needed, by tailoring the driver gas with nitrogen. Before introducing the test gas mixture, the ultimate pressures in the driven section and the mixing tank achieve to be <1 Pa, while the leaking rate is <1 Pa/min. The incident shock velocity was measured using four piezoelectric pressure transducers (PCB 113B26) over the last 1.3 m of the shock tube with the same interval of 300 mm, trigged by three time-counters (FLUKE PM6690) to record the time intervals. The reflected-shock conditions were calculated by a chemical equilibrium software GASEQ[30]. The uncertainty in the reflected temperature was estimated to be ± 20 K using the root-sum square method, and it typically causes ± 20% uncertainty in IDT, based on Arrhenius-type correlation, the details are available in literature[31].

Detailed compositions of the test mixture are listed in Table 1. The purity of methane, oxygen, nitrogen, helium, and argon is 99.99%, 99.999%, 99.999%, 99.999, and 99.999, respectively. The mixture was allowed to homogenize for >12 h to ensure sufficient mixing through free molecular diffusion. Note that nitrogen replaced by argon as the air composition is to minimize the effect of vibration relaxation during the ignition induced period.

2.2. IDT measurement

Two diagnostics were employed: Excited OH (OH*) emission near 307 nm detected by a photomultiplier (HAMAMASSU CR131), and pressure time-history monitored by a piezoelectric pressure transducer with acceleration compensation (PCB 113B03). Both are installed in the end wall of the tube. The IDT is defined as the time interval between the arrival of the incident shock wave at the end wall and the extrapolation of the maximum slope of OH* emission to the

Table 1. Gas mixture compositions in mole fraction

Mixture #	XCH_4/(%)	XO_2/(%)	XAr/(%)	φ	p/(MPa)	T/(K)
1	4.998	19.953	75.049	0.5	1.8	952–1235
2	9.502	19.005	71.493	1.0	1.8	800–1428

φ: Equivalence ratio

baseline, Figure 2. Under these operating conditions, the IDTs defined by the two signals are self-consistent, for either undiluted (Figure 2a) or diluted mixture (Figure 2b). The differences between the both signals are typically within ± 5% at the most test conditions, whereas it can increase to ± 18% when the IDT <100 μs due to the effect of blast wave at high temperatures. It is well known that the interaction between reflected shock wave and boundary layer can induce an obvious pressure rise before the main ignition event[27,28,32]. In this study, however, it is observed a big different pressure rise (dp/dt) in the two typical cases. For the diluted condition, Figure 2a, the non-reactive case shows only 4%/ms of dp/dt, but it reaches 11.8%/ms for the undiluted condition, Figure 2b. The reason causing the big different pressure rise could be attributed to different thickness of the boundary layer due to the difference in viscosity of the test mixtures. In view of the significant effect of pressure rise on model simulation in IDT, over 1.5 ms, in particular, the measured dp/dt (11.8%) has been considered in all calculations in this study.

3. Kinetic model and simulation method

3.1. Simulation approach

Numerical simulations for all experiments were performed by Chemkin-Pro[33] in two ways: (1) Constant ultraviolet (UV) assumption and (2) SENKIN/VITM with considering dp/dt of 11%/ms. Four widely accepted kinetic mechanisms, UBC Mech 2.1[12,19,20], GRI Mech 3.0[21], Aramco Mech 2.0[22-25], and USC Mech 2.0[26], were selected to simulate the measured IDTs. Using extrapolation of maximum pressure rise point back to the baseline was as the modeling IDT. Despite the definitions of measured and simulated IDT were addressed in different ways, it only presented a quite small discrepancy in our previous observation[29]. Figure 3 shows the comparison of IDTs using the constant UV assumption

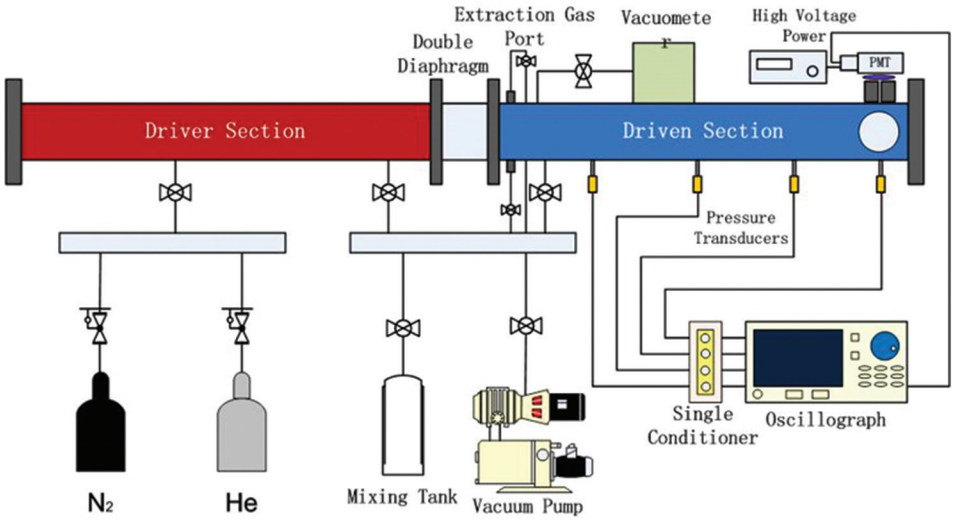

Figure 1. Schematic of the shock tube.

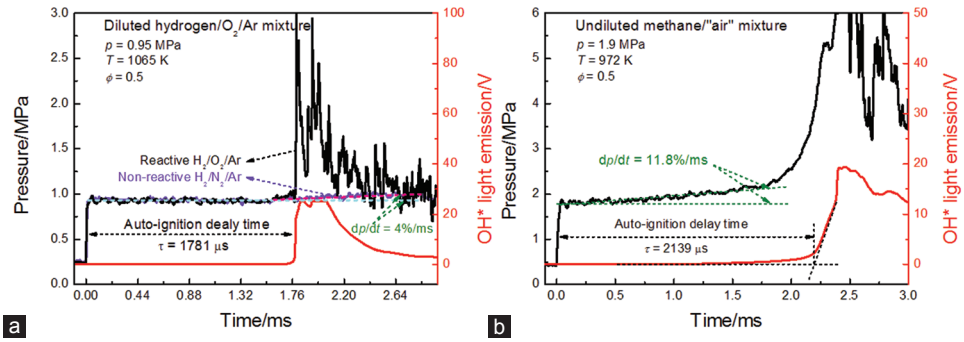

Figure 2. Definition of ignition delay time. (a) Diluted mixture; (b) undiluted mixture.

and SENKIN/VIME for stoichiometric methane/air mixture at 1.8 MPa over 800–1428 K. Clearly, both the simulation approaches show similar predictions only at the temperature over 1110 K. The maximum difference between the two is approximately 18% (1110 K) within the experimental uncertainty. However, it gives a dramatic deviation when the temperature blows 1110 K, and the difference tends to be more apparent with decreasing temperatures. Specifically, the constant UV simulation shows one order of magnitude higher than the SENKIN/VTIM one which is in good agreement with the experimental data. The comparison thus proves, once again, the significance of non-ideal effect caused by the interaction of shock wave and boundary layer, in terms of predicting fuel reactivity at low temperatures corresponding to the longer IDT.

3.2. Chemical kinetic model

To survey the applicability of selected mechanisms in predicting auto-ignition characteristics under typical engine relevant conditions, the new experimental IDT data are compared with the model simulations at 1.8 MPa and at both fuel-lean and fuel-stoichiometric conditions, Figure 4. Qualitatively, the four kinetic mechanisms show an acceptable prediction tendency by considering the effect of pressure rise (11.8%/ms). Quantitatively, only UBC Mech 2.1 captures well the auto-ignition behavior and the others over-predict the reactivity, especially for fuel-stoichiometric mixture at the temperatures of 1000–1250 K. It is no surprise that important species (CH_3O_2, CH_3O_2H, C_2H_5O, $C_2H_5O_2$, $C_2H_5O_2H$, and CH_3CO) relative to low-temperature oxidation of methane did not include in the GRI Mech 3.0 and USC Mech 2.0. In addition, the Aramco Mech 2.0 was validated with the IDTs measured by Petersen *et al.*[10,11] for both diluted and undiluted methane mixtures at high pressures (40–260 atm) and intermediate temperatures (1040–1500 K), but the validation data were mostly focused on fuel-rich (equivalence ratios of 3.0 and 6.0) conditions and did not achieve to lower temperatures (<1040 K). It, thus,

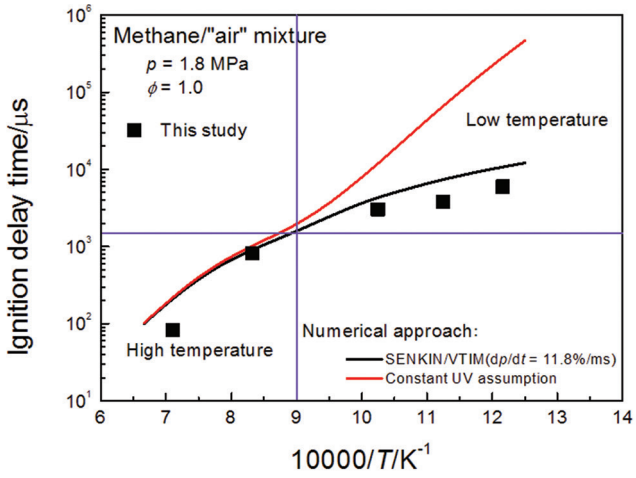

Figure 3. Comparison of SENKIN/VTIM and constant ultraviolet for simulation of undiluted methane/air mixture. UBC Mech 2.1[12,19,20] was adopted for the model predictions.

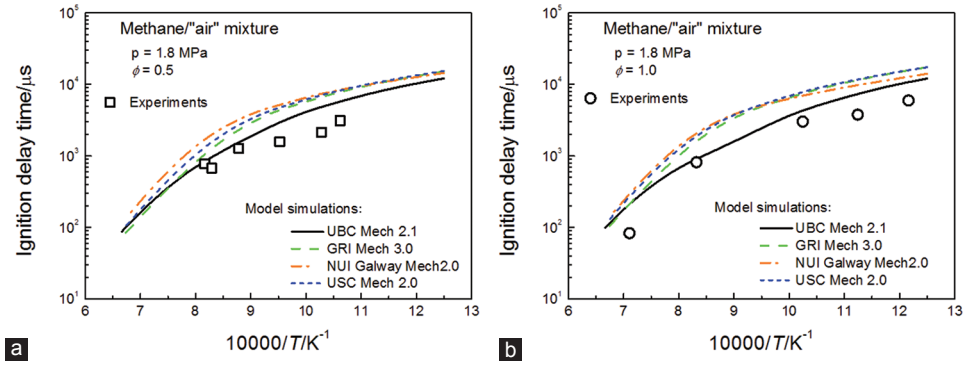

Figure 4. Comparison of experimental and simulated ignition delay times. (a) Fuel-lean condition; (b) fuel-stoichiometric condition.

leads a relatively large deviation from the experimental results under the current conditions. To improve the performance of kinetic mechanism of methane, at high pressure and lower temperatures, in particular, Huang *et al*.[12] modified some of the important elementary reactions identified by sensitivity analysis with incorporating either direct experimental measurements or high-level ab-initio calculations obtained from literature. Specifically, the H-atom abstraction by HO_2 radicals was taken from Hunter *et al*. recommendation[7]. The rate constant for O_2 addition to CH_3 forming CH_3O_2 was adopted from Tsang and Hampson[34]. The sub-set of CH_3O_2 ($CH_3O_2 + HO_2 = CH_3O_2H + O_2$ and $CH_3O_2 + CH_3O_2 = O_2 + CH_3O + CH_3O$) was taken from Curran *et al*. estimations[35]. In general, the UBC Mech 2.1 is capable of capturing the reduction and reincrease in activation energy at lower temperatures as observed in both current and Huang *et al*.[12] studies. Based on it, the UBC Mech 2.1 was chosen for the discussion and kinetic analysis in the next section.

4. Results and discussion

4.1. Transition of deflagration to detonation

Typical auto-ignition process of hydrocarbons is either single stage ignition for non-negative temperature coefficient (NTC) fuels such as ethanol[36] and toluene[37] or two stage ignition for NTC fuels such as n-heptane[38]. However, a novel ignition phenomenon is recognized in the undiluted methane oxidation, Figure 5, where shows the comparison between experimental and simulated pressure-time histories for the stoichiometric mixture at different temperatures. For the high-temperature case (1201 K), the reflected shock pressure increases gradually before the main ignition event; it leads a third stage ignition behavior during the methane oxidation, named deflagration delay (constant pressure), deflagration (gradually increased pressure), and detonation (sharply increased pressure), Figure 5a. However, the simulated pressure shows almost uniform evolution before the main ignition, meaning that the kinetic model is not capable of reproducing the deflagration and detonation processes although it gives a good agreement with the measured total IDT. If moving down the temperature to 822 K, Figure 5b, the reflected shock pressure presents an extra ignition process, named transition of deflagration to detonation transition (DDT), except deflagration delay, deflagration, and detonation. Note that during the DDT transition, the pressure remains constant until the main ignition occurs. Again, the model captures well the total IDT, but it cannot reproduce the four-stage ignition phenomenon. In addition, the deflagration delay time increases with decreasing temperature, and this tendency is consistent with the temperature-dependence of total IDT. Previously, it was mostly focused on the experimental and simulated comparison of IDTs, while it was paid relativity little attention to the auto-ignition process. Current study, therefore, suggests that more efforts on methane oxidation mechanism are needed to better describe the heat release during the auto-ignition process.

4.2. Effect of equivalence ratio

Figure 6 shows the effect of equivalence ratio on the IDTs of methane/air mixtures at 1.8 MPa. In general, the IDT has a negative equivalence ratio dependence for either non-NTC fuels[15,39] or NTC fuels[35,40] at lower temperatures, due to such

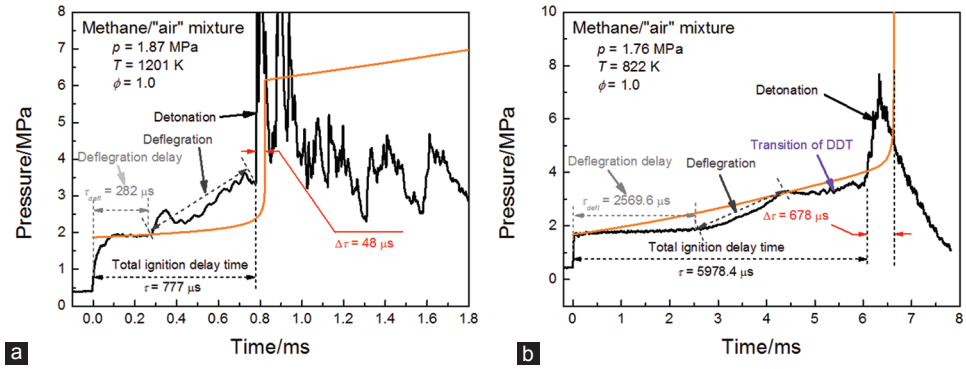

Figure 5. Auto-ignition characteristic of methane/air mixture at a pressure of 1.8 MPa and high temperature (a) and low temperature (b). Solid black line: Pressure trace measured in this study; solid orange line: Model simulation with UBC Mech 2.1[12,19,20].

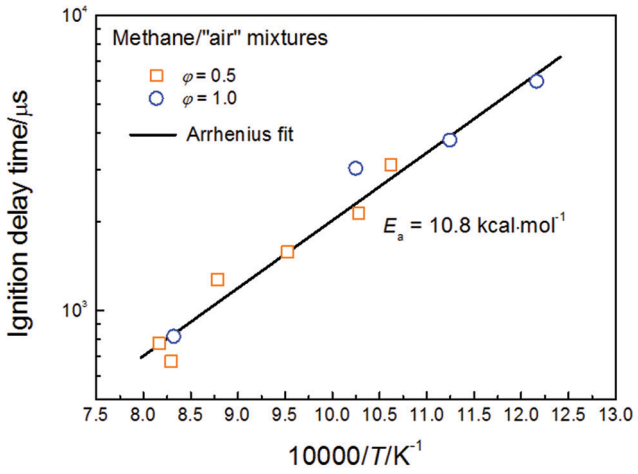

Figure 6. Effect of equivalence ratio on IDT at 1.8 MPa.

the fact that the reactions involving fuel and fuel radicals dominate ignition kinetics. As a result, the rates of elementary reactions involving fuel and fuel radicals enhance due to higher reactant concentration under fuel-rich condition, and it thus accelerates the fuel consumption through increased global reaction rate and shortens the IDTs. In the current study, however, the change in equivalence ratios from 0.5 to 1.0 causes a quite limited effect on the reactivity of methane/air mixtures due to the tiny change in oxygen concentrations. The kinetically interpretation of this behavior is available in the next section. To further verify the negligible dependence of equivalence ratios on the IDTs, an Arrhenius type empirical correlation was fitted through multiple linear regression,

$$\tau = 10.77 \times \varphi^{0.061} \times \exp\left[\frac{-10.8\left(\text{kcal mol}^{-1}\right)}{RT}\right] \quad (1)$$

Where τ is the IDT in microsecond, ϕ is equivalence ratio, T is temperature in Kelvin, and R is the universal gas constant. The goodness of fit, R^2 is 0.97. The global activation energy (E_a) is 10.8 kcal/mol. Note that the exponent of equivalence ratio is approximately 0.06 meaning once again the weak dependence of equivalence ratios on the reactivity of methane/air mixtures under the engine relevant conditions.

4.3. Sensitivity analysis

To identify the key reactions dominating the ignition kinetics in the undiluted methane oxidation, a brute force sensitivity analysis was performed at different temperatures (850 K and 1500 K) and various equivalence ratios (0.5 and 1.0) using UBC Mech 2.1. The sensitivity coefficient is defined as a perturbation caused by a change in A-factor for each reaction rate constant in a common way[28] as follows,

$$S = \frac{\tau(2jk_i) - \tau(0.5k_i)}{1.5(\tau k_i)} \quad (2)$$

Where τ is the IDT, k_i is rate constant of the i^{th} reaction, and S_i is the sensitivity coefficient of i^{th} reaction. A negative value means that the reaction promotes reactivity and vice versa.

Figure 7 illustrates the typical results from the brute force sensitivity analysis for the stoichiometric methane/air mixtures at a pressure of 1.8 MPa in two persuasive cases, high temperature (1500 K), and lower temperature (850 K). The dominant promoting reactions are R155, R119, R38, and R157 at 1500 K. As a general rule, the ignition kinetic is driven by the formation and consumption of the radical pool. The chain termination controlling radicals for the conditions herein are the relatively unreactive CH_3 and HO_2, while the chain branching controlling radicals are H atom, O atom, and OH radical. For the undiluted methane mixture studied in this work, R38 is no longer primarily promoting reaction even at the high temperature (1500 K) relative to previous study[27,28], instead of it, R155 and R119 thoroughly promote the reactivity due to the conversion of relatively low active radicals CH_3 and HO_2 to high active radicals OH and O. In addition, the extra H atoms readily release from the decomposition of CH_3O generated through R155 and R119 and further promote the fuel

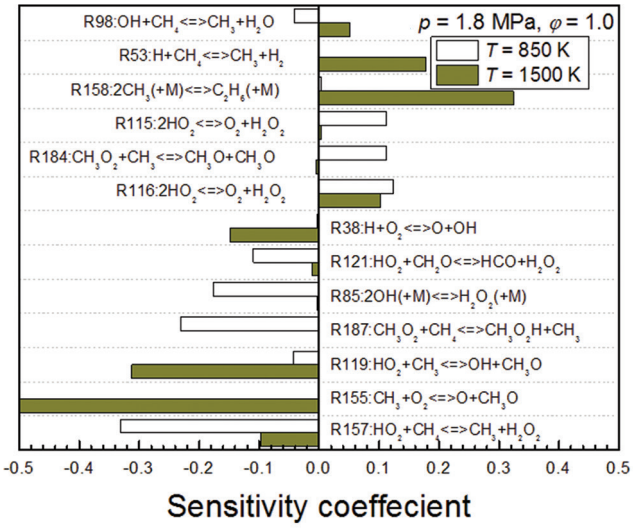

Figure 7. Brute force sensitivity analysis for methane/air mixtures at different temperatures.

reactively. H-atom abstraction of CH_4 by HO_2 through R157 shows a negative sensitivity coefficient, meaning it enhances the CH_4/O_2 ignition, and the similar behavior has also been observed by Golovitchev *et al*.[41].

$$CH_3 + O_2 = O + CH_3O \quad R155$$
$$CH_3 + HO_2 = OH + CH_3O \quad R119$$
$$H + O_2 = O + OH \quad R38$$
$$CH_4 + HO_2 = CH_3 + H_2O_2 \quad R157$$

The primarily inhibiting reactions are R158, R53, and R116. Among them, the most important reaction is a recombination of CH_3 through R158, which serves as a sink for CH_3 radicals driving chain termination. Second inhibiting reaction is H atom abstraction of CH_4 through R53 due to the conversion of active H atom to unreactive CH_3 radicals. Visually, the increased negative effect of R116 on reactivity appears contradictory due to H_2O_2 formation followed by its decomposition to two OH radicals through R-85. However, in fact, R116 competes for HO_2 radicals with the more substantial HO_2 formation channel R157 as well as the more efficient use of HO_2 through R119. As mentioned above, the channels R119 and R157 are second and fourth promoting reactions, respectively, and the competition is clear to inhibit the auto-ignition process and lengthen the IDT.

$$CH_3 + CH_3 (+M) = C_2H_6 (+M) \quad R158$$
$$CH_4 + H = CH_3 + H_2 \quad R53$$
$$HO_2 + HO_2 = O_2 + H_2O_2 \quad R115/R116$$

When the temperature reduces to 850 K, the dominating reactions change significantly. The ignition controlling reactions are R157, R187, R-85, and R121.

$$CH_4 + CH_3O_2 = CH_3O_2H + CH_3 \quad R187$$
$$H_2O_2 (+M) = 2OH (+M) \quad R-85$$
$$CH_2O + HO_2 = HCO + H_2O_2 \quad R121$$

The stable formaldehyde (CH_2O) formed by decomposition of CH_3O radicals is also converted to active HCO and H_2O_2 through R121, it, thus, enhances the reactivity. Note that the depletion of CH_3 mainly undergoes O_2 addition reaction forming CH_3O_2 through R179.

$$CH_3 + O_2 (+M) = CH_3O_2 (+M) \quad R179$$

The CH_3O_2 radicals become an important carrier except for CH_3 and HO_2 radicals at lower temperatures. As a result, the majority of CH_4 is consumed through H atom abstraction reaction by CH_3O_2 through R187, which converts the stable CH_3O_2 to active CH_3O_2H and thus accelerates methane ignition. Regarding the ignition inhibitors, R53 and R158 no longer control the ignition due to the relatively high energy barriers and less H atoms. In contrast, R184 and R115 show quite weak sensitivity at high temperatures, largely attribute the inhibiting effect on the reactivity of methane

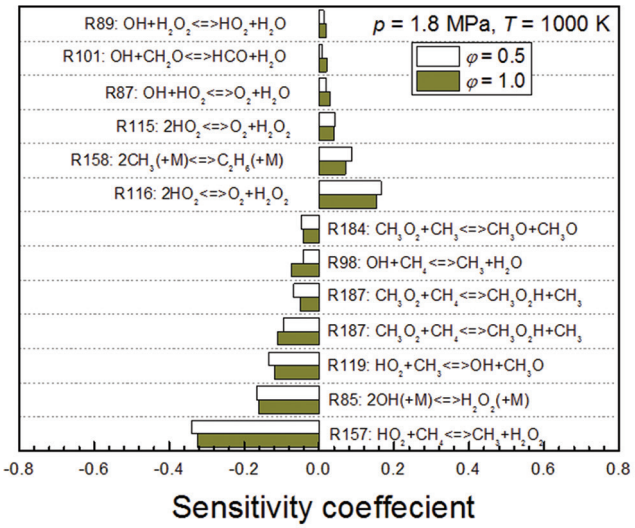

Figure 8. Brute force sensitivity analysis for methane/air mixtures at various equivalence ratio.

due to the formation of two active CH_3O radicals. The sensitivity coefficient of R116 is generally no change at various temperatures.

$$CH_3O_2 + CH_3 = CH_3O + CH_3O \qquad R184$$

In this study, reduced global activation energy with decreasing temperature was observed (Figure 4) and the similar behavior was also obtained from Petersen *et al*.[10] work at higher pressure (260 atm). To explore the transition of activation energy, we analyze the difference in the ignition kinetics at 850 K and 1500 K. For the high temperatures, substantial H and O atoms are accumulated through R155 and R119 followed by R38 to accelerate the chain branching process. For the lower temperature, however, OH radicals are largely generated from H_2O_2 direct decomposition through R-85. Moreover, R157 and R121 are main contributors to the formation of H_2O_2. The branching effect caused by the increase of OH concentration markedly enhances fuel consumption. The influence is elevated with decreasing temperatures, and it thus explains the trends evident in the global activation energy. Note that R184 and R187 are competitive reactions for CH_3O_2 radicals while the latter one tends to be dominant in the competition with decreasing temperatures. It further makes help to reduce the activation energy. However, the current kinetic analysis does not fully interpret the chemistry during the multistage ignition process of the undiluted methane, and it remains the topics for further consideration.

To verify the limited effect of equivalence ratios on the IDTs measured in this study, the brute force sensitivity analysis was carried out for the mixtures with various equivalence ratios, fuel-lean (ϕ = 0.5), and fuel-stoichiometric (ϕ = 1.0), at fixed temperature (1000 K) and pressure (1.8 MPa), Figure 8. It can be seen that the dominant reactions are similar to the analysis above. Yet, the change in equivalence ratio does not cause an evident increase or decrease in the significance of the highlighted reactions, meaning the ignition controlling factors remain the same way under fuel-lean and fuel-stoichiometric conditions in the undiluted methane oxidation. In fact, the most important promoter and inhibitor are R157 and R116, respectively. The key initiator driving these two reactions is HO_2 radical. The change in equivalence ratio from 0.5 to 1.0 only causes a little float of oxygen concentration from 19.95% to 19%. It means that the help to HO_2 accumulation through R36 is almost the same for the methane/air mixtures at various equivalence ratios. It is constant with the experimental observation, Figure 6.

$$CH_3O_2 + CH_3 = CH_3O + CH_3O \qquad R36$$

5. Concluding remark

Shock tube experiments on methane/air ignition were performed under engine relevant conditions covering the temperature range of 800–1428 K and equivalence ratios of 0.5 and 1.0 at a pressure of 1.8 MPa. Undiluted mixtures show outstanding high-pressure rise (11.8%/ms) relative to the diluted case. OH* light emission diagnostic demonstrates that the cause stems from the interaction between the reflected shock wave and boundary layer rather than pre-ignition

energy release. Two types of multistage ignition, deflagration delay/deflagration/detonation at higher temperatures and deflagration delay/deflagration/DDT transition/detonation at lower temperatures are identified during the oxidation of methane/air mixtures. The IDTs do not show sensitive to the change of equivalence ratio, and this behavior is proved through the fitted Arrhenius empirical correlation.

Four chemical kinetic mechanisms, UBC Mech 2.1, GRI Mech 3.0, Aramco Mech 2.0, and USC Mech 2.0, were adopted to simulate the measured IDTs. Considering the dp/dt of 11.8%/ms, only UBC Mech 2.1 shows an acceptable agreement with the new data due to its complete low-temperature chemistry. Nevertheless, the UBC Mech 2.1 is still not capable of predicting the multistage ignition. Sensitivity analysis indicates that, in general, the sensitivity coefficients of dominant reactions are more sensitive to temperature relative to equivalence ratio. It shows the evident difference in chain branching processes at different temperatures. For high temperatures, the chain branching is mainly driven by initiator H atom formed from R155 and R119 followed by OH radicals accumulation through R38. For lower temperatures, however, the OH radicals are mainly driven by initiator H_2O_2 radicals generated from H-atom abstraction reactions of CH_4 and CH_2O by HO_2 radicals, followed by H_2O_2 decomposition through R-85. More evident chain branching effect at lower temperatures contributes to the lower activation energy. The chemical kinetic explanation on the multistage ignition is needed to further understand the nature of undiluted methane auto-ignition.

Acknowledgment

Research reported in this publication was funded by the National Natural Science Foundation of China (91841301 and 91741115) and Shanxi National Science Foundation (2018JC-002).

References

1. Semin R A B, 2008, A technical review of compressed natural gas as an alternative fuel for internal combustion engines. *Am J Eng Appl Sci*, 1: 302–311. https://doi.org/10.3844/ajeassp.2008.302.311.
2. Lefebvre A H, 1998, *Gas Turbine Combustion*. Boca Raton: CRC Press.
3. Hertzberg A, Bruckner A, Bogdanoff D, 1988, Ram accelerator–a new chemical method for accelerating projectilesto ultrahigh velocities. *AIAA J*, 26: 195–203. https://doi.org/10.2514/3.9872.
4. Spadaccini L, Colket M 3rd, 1994, Ignition delay characteristics of methane fuels. *Prog Energy Combust Sci*, 20: 431–460. https://doi.org/10.1016/0360-1285(94)90011-6.
5. Cheng R, Oppenheim A, 1984, Autoignition in methane hydrogen mixtures. *Combust Flame*, 58: 125–139. https://doi.org/10.1016/0010-2180(84)90088-9.
6. Petersen E L, Röhrig M, Davidson D F, *et al*., 1996, *High-pressure Methane Oxidation Behind Reflected Shock Waves*. Symposium (International) on Combustion. Elsevier. p799–806. https://doi.org/10.1016/S0082-0784(96)80289-X.
7. Hunter T, Wang H, Litzinger T, *et al*., 1994, The oxidation of methane at elevated pressures: Experiments and modeling. *Combust Flame*, 97: 201–224. https://doi.org/10.1016/0010-2180(94)90005-1.
8. Li S, Williams F, 2000, Reaction mechanisms for methane ignition. In: *ASME Turbo Expo 2000: Power for Land, Sea, and Air*. New Orleans, Louisiana: American Society of Mechanical Engineers. pV002T002A061–V002T002A061. https://doi.org/10.1115/2000-GT-0145.
9. Hidaka Y, Sato K, Henmi Y, *et al*., 1999, Shock–tube and modeling study of methane pyrolysis and oxidation. *Combust Flame*, 118: 340–358. https://doi.org/10.1016/S0010-2180(99)00010-3.
10. Petersen E, Davidson D, Hanson R, 1999, Kinetics modeling of shock–induced ignition in low–dilution CH4/O2 mixtures at high pressures and intermediate temperatures. *Combust Flame*, 117: 272–290. https://doi.org/10.1016/S0010-2180(98)00111-4.
11. Petersen E L, Davidson D F, Hanson R K, 1999, Ignition delay times of Ram accelerator CH/O/diluent mixtures. *J Propulsion Power*, 15: 82–91. https://doi.org/10.2514/2.5394.
12. Huang J, Hill P, Bushe W, *et al*., 2004, Shock–tube study of methane ignition under engine–relevant conditions: experiments and modeling. *Combust Flame*, 136: 25–42. https://doi.org/10.1016/j.combustflame.2003.09.002.
13. De Vries J, Petersen E, 2007, Autoignition of methane–based fuel blends under gas turbine conditions. *Proc Combust Inst*, 31: 3163–3171. https://doi.org/10.1016/j.proci.2006.07.206.
14. Petersen E L, Hall J M, Smith S D, *et al*., 2007, Ignition of lean methane–based fuel blends at gas turbine pressures. *J Eng Gas Turbine Power*, 129: 937–944. https://doi.org/10.1115/1.2720543.

15. Healy D, Curran H, Simmie J, *et al*., 2008, Methane/ethane/propane mixture oxidation at high pressures and at high, intermediate and low temperatures. *Combust Flame*, 155: 441–448. https://doi.org/10.1016/j.combustflame.2008.07.003; https://doi.org/10.1016/j.combustflame.2008.06.008.
16. Herzler J, Naumann C, 2009, Shock–tube study of the ignition of methane/ethane/hydrogen mixtures with hydrogen contents from 0% to 100% at different pressures. *Proc Combust Inst*, 32: 213–220. https://doi.org/10.1016/j.proci.2008.07.034.
17. Herzler J, Naumann C, 2012, Shock tube study of the influence of NOx on the ignition delay times of natural gas at high pressure. *Combust Sci Technol*, 184: 1635–1650. https://doi.org/10.1080/00102202.2012.690617.
18. El Merhubi H, Kéromnès A, Catalano G, *et al*., 2016, A high pressure experimental and numerical study of methane ignition. *Fuel*, 177: 164–172. https://doi.org/10.1016/j.fuel.2016.03.016.
19. Huang J, Bushe W, Hill P, *et al*., 2006, Experimental and kinetic study of shock initiated ignition in homogeneous methane–hydrogen–air mixtures at engine-relevant conditions. *Int J Chem Kinet*, 38: 221–233. https://doi.org/10.1002/kin.20157.
20. Huang J, Bushe W, 2006, Experimental and kinetic study of autoignition in methane/ethane/air and methane/propane/air mixtures under engine–relevant conditions. *Combust Flame*, 144: 74–88. https://doi.org/10.1016/j.combustflame.2005.06.013.
21. Smith G P, Golden D M, Frenklach M, *et al*., 2000, *GRI-Mech 3.0*. Available from: http://www.me.%20berkeley.%20edu/gri_mech.
22. Metcalfe W K, Burke S M, Ahmed S S, *et al*., 2013, A hierarchical and comparative kinetic modeling study of C1− C2 hydrocarbon and oxygenated fuels. *Int J Chem Kinet*, 45: 638–675. https://doi.org/10.1002/kin.20802.
23. Kéromnès A, Metcalfe W K, Heufer K A, *et al*., 2013, An experimental and detailed chemical kinetic modeling study of hydrogen and syngas mixture oxidation at elevated pressures. *Combust Flame*, 160: 995–1011. https://doi.org/10.1016/j.combustflame.2013.01.001.
24. Burke S M, Burke U, Mc Donagh R, *et al*., 2015, An experimental and modeling study of propene oxidation. Part 2: Ignition delay time and flame speed measurements. *Combust Flame*, 162: 296–314. https://doi.org/10.1016/j.combustflame.2014.07.032.
25. Burke S M, Metcalfe W, Herbinet O, *et al*., 2014, An experimental and modeling study of propene oxidation. Part 1: Speciation measurements in jet–stirred and flow reactors. *Combust Flame*, 161: 2765–2784. https://doi.org/10.1016/j.combustflame.2014.05.010.
26. Wang H, You X, Joshi A V, *et al*., 2007, *USC Mech Version II, High–Temperature Combustion Reaction Model of H 2 Program*. p96.
27. Zhang Y, Jiang X, Wei L, *et al*., 2012, Experimental and modeling study on auto–ignition characteristics of methane/hydrogen blends under engine relevant pressure. *Int J Hydrogen Energy*, 37: 19168–19176. https://doi.org/10.1016/j.ijhydene.2012.09.056.
28. Zhang Y, Huang Z, Wei L, *et al*., 2012, Experimental and modeling study on ignition delays of lean mixtures of methane, hydrogen, oxygen, and argon at elevated pressures. *Combust Flame*, 159: 918–931. https://doi.org/10.1016/j.combustflame.2011.09.010.
29. Zhang J, Niu S, Zhang Y, *et al*., 2013, Experimental and modeling study of the auto–ignition of n–heptane/n–butanol mixtures. *Combust Flame*, 160: 31–39. https://doi.org/10.1016/j.combustflame.2012.09.006.
30. Morley C, 2005, *Gaseq: A Chemical Equilibrium Program for Windows*, Version 0.79.
31. Deng F, Yang F, Zhang P, *et al*., 2016, Towards a kinetic understanding of the NOx promoting–effect on ignition of coalbed methane: A case study of methane/nitrogen dioxide mixtures. *Fuel*, 181: 188–198. https://doi.org/10.1016/j.fuel.2016.04.090.
32. Davidson D F, Hanson R K, 2004, Interpreting shock tube ignition data. *Int J Chem Kinet*, 36: 510–523. https://doi.org/10.1002/kin.20024.
33. Reaction Design, Inc, 2011, *CHEMKIN–PRO, 15112*. San Diego, CA: Reaction Design, Inc.
34. Tsang W, Hampson R, 1986, Chemical kinetic data base for combustion chemistry. Part I. Methane and related compounds. *J Phys Chem Ref Data*, 15: 1087–1279. https://doi.org/10.1063/1.555759.
35. Curran H, Fischer S, Dryer F, 2000, The reaction kinetics of dimethyl ether. II: Low-temperature oxidation in flow reactors. *Int J Chem Kinet*, 32: 741–759. https://doi.org/10.1002/1097-4601(2000)32:12<741:AID-KIN2>3.0.CO;2-9.
36. Zhang Y, El-Merhubi H, Lefort B, *et al*., 2018, Probing the low–temperature chemistry of ethanol via the addition of dimethyl ether. *Combust Flame*, 190: 74–86. https://doi.org/10.1016/j.combustflame.2017.11.011.
37. Zhang Y, Somers K P, Mehl M, *et al*., 2017, Probing the antagonistic effect of toluene as a component in surrogate

fuel models at low temperatures and high pressures. A case study of toluene/dimethyl ether mixtures. *Proc Combust Inst*, 36: 413–421. https://doi.org/10.1016/j.proci.2016.06.190.
38. Zhang K, Banyon C, Bugler J, *et al*., 2016, An updated experimental and kinetic modeling study of n–heptane oxidation. *Combust Flame*, 172: 116–135. https://doi.org/10.1016/j.combustflame.2016.06.028.
39. Shen H P S, Vanderover J, Oehlschlaeger M A, 2009, A shock tube study of the auto–ignition of toluene/air mixtures at high pressures. *Proc Combust Inst*, 32: 165–172. https://doi.org/10.1016/j.proci.2008.05.004.
40. Curran H J, Gaffuri P, Pitz W J, *et al*., 1998, A comprehensive modeling study of n–heptane oxidation. *Combust Flame*, 114: 149–177. https://doi.org/10.1016/S0010-2180(97)00282-4.
41. Golovitchev V, Pilia M, Bruno C, 1996, Autoignition of methane mixtures–the effect of hydrogen peroxide. *J Propulsion Power*, 12: 699–707. https://doi.org/10.2514/3.24091.